Progress In Electromagnetics Research C, Vol. 94, 203–217, 2019

Circularly Polarized Array Antenna Using the Sequential Rotation Network Feeding for X-Band Communication

Farohaji Kurniawan[*, 1, 2], Josaphat Tetuko Sri Sumantyo[1], Koichi Ito[3], Steven Gao[4], Good Fried Panggabean[1], and Gunawan Setyo Prabowo[2]

Abstract—This paper presents a novel Circularly Polarized (CP) microstrip array antenna with circular shape and slotted by an elliptical ring for X-band communication. This array antenna consists of 4 paths. Each patch is designed with a unique model, and the purposed antenna is mainly circular-shaped. An elliptical ring slot is set at the center of the circular-shaped patch. And a pair of triangle shapes employed as truncation factor is placed at the edge of the circular-shaped antenna. This microstrip array antenna is developed by 2×2 patches in a sequential rotation mode with relative phases 0°, 90°, 180°, and 270°. The total dimension of this array antenna is 60.92 mm × 60.92 mm. The simulated result shows a good agreement with minimum requirement. The center frequency of the antenna design is 8.2 GHz with low frequency at 8 GHz and high frequency at 8.4 GHz. The proposed antenna is produced under −10 dB S_{11} of 21.9%, maximum gain of 12.47 dBic at the center frequency, and axial ratio bandwidth of 12.2% is obtained. Simulated result has been validated by fabrication and measurement, then the structure of the antenna design is fabricated on NPC-H22A with a thickness of 1.6 mm and dielectric constant of 2.17. Complete investigation and experimentation are presented in the next sections.

1. INTRODUCTION

In the last decade, microstrip antenna has attracted earnest consideration of the antenna community [1]. Due to its dependability of compactness, easy fabrication, low profile, light weight, portability, and low cost fabrication [2], microstrip antenna is very suitable for the requirement of satellite (space-borne) [3] and air-borne applications [4, 5]. Furthermore, microstrip antenna significantly has flourished in some field, for example, military [6], medical [7], and maritime [8] fields. Thus, the development of a circularly polarized (CP) antenna for X-band communication utilizes microstrip material. The development of the antenna is based on GAIA II/LAPAN-Chiba-sat project. LAPAN-Chibasat is a collaborative project between Josaphat Microwave and Remote Sensing Laboratory (JMRSL) of Chiba University and National Institute Aeronautics and Space of Indonesia (LAPAN) [9]. GAIA II/Chiba-sat is planned to be launched in 2022. GAIA II/Chiba-sat is a Synthetic Aperture Radar (SAR) satellite with an L-band CP-SAR antenna which is employed as the sensor. This GAIA II has a total mass of 150 kg. Also this antenna communication could be implemented on air-borne vehicles (UAV, quad-rottor) [10].

Low gain is one of the drawbacks of the microstrip antenna [11–15]. Therefore, various possible solutions were attempted to rectify this issue, for example, utilizing a near-zero-index meta-material to enhance the gain [16]. Nevertheless, its structure was excessively fragile. The second solution was using a

Received 17 May 2019, Accepted 18 July 2019, Scheduled 31 July 2019

* Corresponding author: Farohaji Kurniawan (farohaji.kurniawan@lapan.go.id).

[1] Josaphat Microwave Remote Sensing Laboratory, Center for Environmental Remote Sensing Graduate School Advanced Integration Science, Chiba University, Chiba, Japan. [2] Center for Aeronautics Technology, National Institute of Aeronautics and Space, Bogor, Indonesia. [3] Research Center for Frontier Medical Engineering, Inage, Chiba University. [4] School of Engineering and Digital Arts, University of Kent, Canterbury, CT2 7NT, United Kingdom.

cylindrical shell-shaped superstrate [17]. By using this method, the cylindrical shell-shaped superstrate material is set on a patch radiator. This method succeeded in increasing gain. However, the result shows that its construction is not rigid and lack of compactness. Another technique was using a single dielectric superstrate on its design [18]. This method implemented a superstrate between two substrates, and it shows that the model is neither compact nor rigid. These three methods showed a similar result that they were all fragile. Another technique in enhancing the bandwidth was by incorporating a phased array method into the design. By employing this technique, the antenna design was kept rigid, compact, and suitable for fast-moving vehicles (such as microsatellite, aircraft, and, UAV). Therefore, the design of the microstrip array antenna with sequential rotation method for X-band communication is presented in this paper.

Furthermore, the design of the single microstrip antenna merely produced 6.5 dBic of gain, whereas the desired gain of the antenna design must be up to 10 GHz and 400 MHz of bandwidth. One of the solutions to rectify this issue was by implementing the antenna array method. This method was already presented in some researches [19, 20]. In addition, the gain of the simulated result reached 6.9 dBic at the center frequency of the single patch. Meanwhile, by using a 2×2 microstrip array method, the gain of the antenna design reached up to 12 dBic at the center frequency (8.2 GHz).

Based on an integral feed network, the array antenna can be divided into corporate feeds and parallel feeds [21]. In comparison, the corporate feeds have better efficiency than the parallel feeds. However, the parallel feeds are more effective in controlling the aperture distribution [22]. In this antenna design, a parallel feed with sequential network feed was employed; 0°, 90°, 180°, and 270° phase shifts were applied to each microstrip. The purposive network feeding design with subsequent rotation is designed to improve circular polarization. This has been presented in many papers, such as in [23–26]. Then a pair of triangle truncation shapes is set at $-45°$ of the x-axis and 45° of the y-axis to generate circular polarization. Meanwhile, an elliptical-ring-slot (ERS) set in the middle of the patch antenna was intended to enhance the bandwidth of the axial ratio and return loss [27].

The minimum requirement of the antenna design presented in Table 1. The antenna design must be in circular polarization mode, with minimum gain up to 10 dBic, total weight of the antenna no more than 0.4 kg, etc. This minimum requirement of the antenna design is based on the RF system of the GAIA II/Lapan chiba-sat. The proposed antenna was printed on double layers. The design of the antenna was simulated in CST Studio Suite 2017. The simulation results showed that bandwidth of return loss obtained 21.9% (7.5–9.3 GHz); <3 dB axial ratio bandwidth achieved 12.2% (7.3–8.3 GHz); and the gain yielded of 12.45 dBic.

Table 1. Minimum requirement of the antenna design.

Parameter	**Specification**	**Units**
Frequency	8.0 to 8.4	GHz
VSWR	≤ 2	
Polarization (T_x/R_x)	Left-handed circular polarization	
Axial ratio (AR)	≤ 3	dB
Return loss	≥ 10	dB
Gain	≥ 10	dBic
Weight	< 0.4	kg
Thickness	< 10	mm
Temperature (°C)	-50 to $+55$	
Operating altitude	550–800	km
Vibration	14	grms

2. SINGLE MICROSTRIP ANTENNA DESIGN

The structure of the single microstrip of the antenna design is shown in Figure 1.

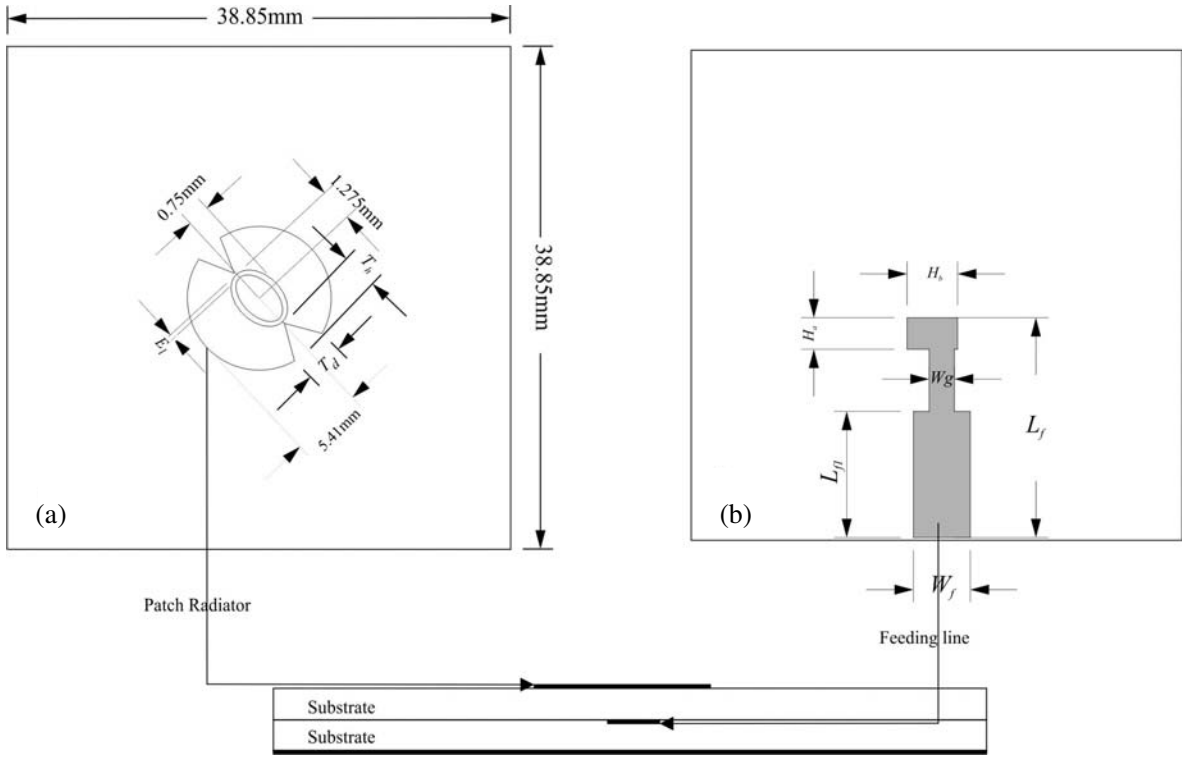

Figure 1. Detail antenna configuration, which there are three parts; (a) Patch side of the antenna, (b) feeding line, and antenna design from the side view.

The antenna is printed in double substrates, on which the first substrate is set for a microstrip radiator, then the back side of top substrate is set for microstrip line and ground-plane set on the second substrate. A patch radiator of the antenna formed by a circular-disk with an elliptical ring slot is set on the centre of the microstrip radiator, while a pair of triangle truncation shapes cuts off the microstrip radiator. The purpose of the truncation factor is to generate polarization characteristics. In addition, the elliptical-ring-slot is another factor that is utilized to strengthen the circularly polarized characteristics and also fashioned as a bandwidth enhancer. As shown in Figure 1, the dimension of single microstrip of the proposed antenna is 38.85 mm $\times L_p = 38.85$ mm is as width and length of the single microstrip antenna. The microstrip radiator of the antenna is represented by $R_p = 5.41$ mm as radius of the circular disk, $R_e = 1.275$ mm as far radius of the elliptical ring slot, and $r_e = 0.775$ mm as a near radius of the elliptical ring slot. The elliptical ring slot has a width about $E_l = 0.22$ mm. The dimension of the triangular truncation is represented by $T_d = 1.5$ mm as width of the triangle and $T_h = 1.6$ mm as height of the triangle. Then for the feeding line $W_f = 4.5$ mm, $W_g = 2$ mm, $L_{fl} = 10$, $L_f = 18$, $H_a = 3$ mm, $H_s = 4$ mm.

2.1. Characteristics of Single Microstrip Antenna

In order to ensure reliability of the antenna design, investigation of characteristics of single microstrip of the proposed antenna is necessary. Four consecutive images in Figure 2 depict typical current distributions on the surface of the single microstrip of the proposed antenna. Undoubtedly, the microstrip antenna design could generate circular polarization characteristics. The SMA connector delivered current from the source to the feed-line. It is shown in Figure 2(1) that the feed-line contains

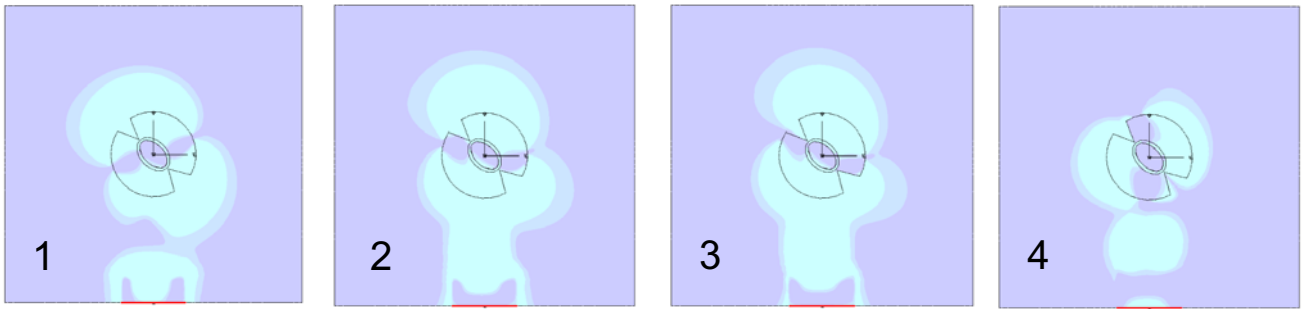

Figure 2. Simulation of surface current distribution on a microstrip antenna.

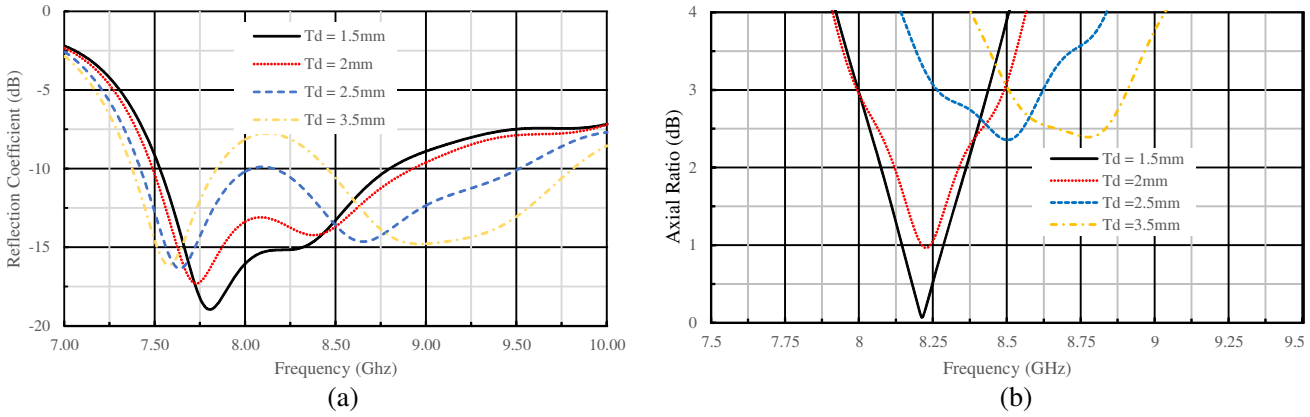

Figure 3. (a) Reflection coefficient, S_{11} of single microstrip antenna; (b) Axial ratio bandwidth of single microstrip antenna.

current and starts to discharge the current. Figure 2(2) depicts that current is transferred to microstrip radiator, flies along the feed-line, then reaches the radiator. The compiled current by the microstrip radiator becomes a wave with circular polarization, which is described in Figures 2(3, 4).

The single microstrip antenna design produced a decent bandwidth of axial ratio, reflection coefficient, S_{11}, and gain. Its result met the minimum requirement of the single microstrip antenna. The simulated result of under -10 dB reflection coefficient, S_{11} bandwidth, reaches 1.2 GHz (7.5–8.7 GHz), with the deepest curve at 7.8 GHz of -18.9 dB, and at the center frequency of 8.2 GHz it is 15.2 dB. The result of the simulated reflection coefficient is shown in Figure 3(a). Then Figure 3(b) depicts the simulated result of < 3 dB axial ratio, and its bandwidth is 0.5 GHz (7.9–8.4 GHz), then the deepest curve at frequency 8.21 GHz is 0.07 dB. The most influential parameter to the circular polarization characteristics is the truncation factor. Detailed comparison result of the triangle shaped truncation variation is as shown in Table 2.

Table 2. Influences of the truncation factor to the antenna characteristics.

Width of T_d (mm)	**Reflection Coefficient (GHz)**	**<3 dB Axial Ratio BW (dB), %**	**Deepest curve of AR (GHz), (dB)**	**Gain (dBic)**
1.5	7.5–8.8	7.9–8.4, 6.7%	8.2, 0.037	6.7 to 6.3
2	7.4–8.9	7.9–8.5, 7.3%	8.2, 1.06	6.8 to 6.4
2.5	7.4–8.02 and 8.17–9.5	8.2–8.6, 4%	8.5, 2.3	6.8 to 6.3
3.5	7.2–7.8 and 8.4–9.8	8.5–8.9, 4%	8.7, 2.4	6.6 to 6.4

Table 2 shows that triangular truncation has a significant effect on circular polarization characteristics. It is an evidence that wider truncation factor will shift the < 3 dB axial ratio to a higher frequency ,and the polarization becomes elliptical. As a result, the axial ratio achievement gets closer to < 3 dB. When $T_d = 1.5$ mm, the axial ratio bandwidth achieved 6.7% with the deepest curve at the center frequency of 8.2 GHz at 0.037 dB, which is close to 0 dB, meaning that it is perfectly circularly polarized. $T_d = 2$ mm also attained good result about 11.6%; nevertheless in the center frequency, it attained about 1.06 dB. Thus, the axial ratio performance of $T_d = 1.5$ mm is better than $w_d = 2$ mm.

On the other result, $T_d = 2.5$ mm and 3.5 mm evince that the axial ratio performance is unsatisfactory. The axial ratio shifted to the higher frequency, up to 8.2 GHz, whereas the desired frequencies were at 8 GHz to 8.4 GHz. Thus, this result is unacceptable. Furthermore, the triangular truncation affects the performances of reflection coefficient, S_{11}. The diversity of the reflection coefficient result can also be seen in Table 2. The widest impedance bandwidth achieved is $T_d = 2$ mm which is able to obtain 18%. Nonetheless, the result reaching the center frequency is low, about 13.5 dB close to -10 dB. $T_d = 2.5$ mm and 3.5 mm can produce dual-band frequency, for 2.5 mm at frequencies of 7.4–8.02 GHz and 8.17–9.5 GHz, then for 3.5 mm at frequencies of 7.2–7.8 GHz and 8.4–9.8 GHz. These results are unacceptable since they are shifted from desired frequency. Then for $T_d = 1.5$ mm can produce good performance of under -10 dB impedance bandwidth which is obtained 18%, and at the center frequency of 8.2 GHz, 15.6 dB is obtained. In conclusion, $T_d = 1.5$ mm is much better in improving the performance of the axial ratio bandwidth and impedance bandwidth among others.

Figure 4 shows the simulated gain of the single microstrip antenna for $T_d = 1.5$ mm. It can be concluded that the variation of the truncation factor has small effect on bandwidth. The gain is 6.68 dBic at the center frequency. Then, at the low frequency (8 GHz) it is 6.7 dBic, and at the high-frequency (8.4 GHz) it is 6.4 dBic. The greatest achievement is at 8.1 GHz of 6.8 dBic. Overall, the expected achievement of gain of the single microstrip antenna is satisfying.

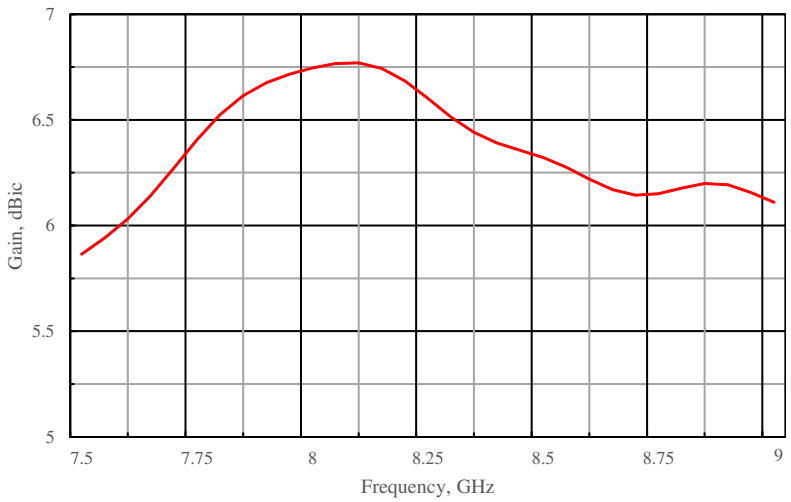

Figure 4. Simulated result of the gain of single microstrip antenna.

3. 2×2 ARRAY ANTENNA DESIGN

Development of the 2×2 array antenna is based on the single microstrip X-band antenna design. The proposed array antenna is developed in a sequential rotation method as illustrated in Figure 5.

This X-band communication antenna has center frequency at 8.2 GHz. A clockwise sequential rotation technique is implemented on this antenna array design. The purpose of this method is to enhance the bandwidth of the axial ratio. The microstrip radiators are separated by a distance of 27 mm or equal to $0.75\lambda_{8.2}$ GHz. The proposed antenna is constructed in double substrates, which is similar to the construction model of the single microstrip one. Thus, the top layer of the substrate is set for microstrip radiator, while the microstrip network feeding is squeezed between the two substrates.

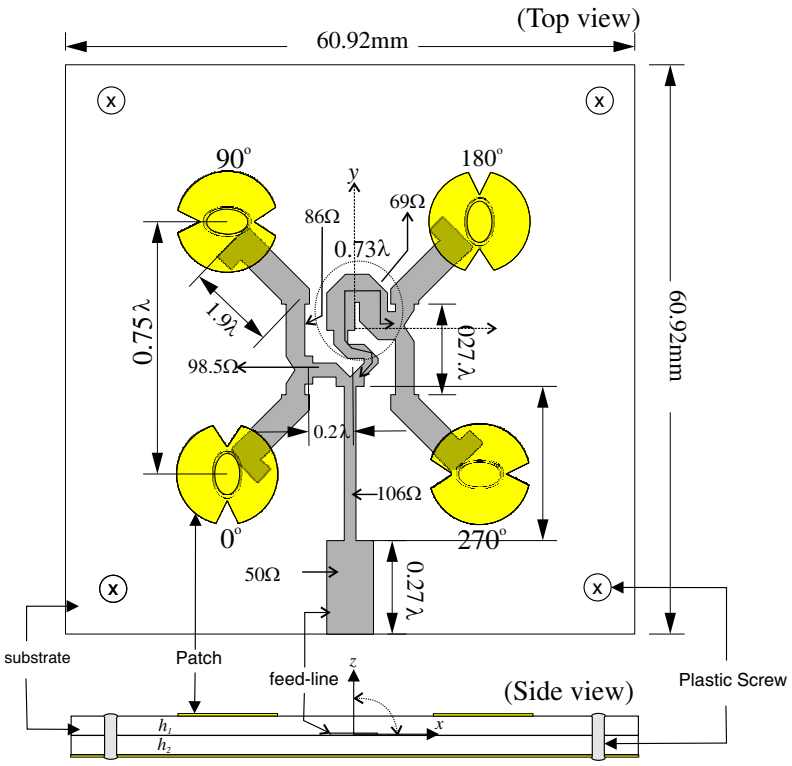

Figure 5. Geometry of the 2×2 sequentially rotated of CP antenna array.

After that, it is set in the backside of the second substrate set for ground-plane. Detailed geometry of the 2×2 array antenna is shown in Figure 5.

Figure 6(a) depicts the comparison of the simulated results of reflection coefficient between single and array antennas. In comparison, the reflection coefficient, S_{11}, of single microstrip antenna is narrower than array's reflection coefficient. The achievement of simulated result of impedance bandwidth of the single microstrip antenna reaches nothing but 15.4% with inmost deep impedance bandwidth at 7.76 GHz of -18 dB. Then at the center frequency reflection coefficient, S_{11}, is -16 dB. On the other hand, the simulated result of reflection coefficient of the array antenna is wider and deeper. Its reflection coefficient result is 21.9% with inmost deep point at 8.51 GHz of -22 dB. Then at the center frequency (8.2 GHz) reflection coefficient, S_{11}, reaches -17 dB.

Comparison of the simulated axial ratios of single microstrip and array antennas is shown in Figure 6(b). Its result shows a significant level of circularly polarized characteristics. The array antenna can produce board-band bandwidth of the axial ratio compared to the axial ration of single microstrip antenna. However, the axial ratio of the single microstrip antenna is sharper than the axial ratio of array antenna. In addition, a single microstrip antenna produced < 3 dB bandwidth of axial ratio which reaches nothing but 6.7% (7.9–8.43 GHz) and tapered at 8.2 GHz of 0.037 dB. Meanwhile, < 33 dB bandwidth of the axial ratio of the array antenna obtains 13% (7.3–8.4 GHz), with inmost deep point at 7.51 GHz of 0.21 dB. Then, at the center frequency it is 1.68 dB. It can be concluded that S_{11} and axial ration bandwidth of the array are wider than single patch. The array antenna has 4 elements radiators which can strengthen radiation power of the antenna. Thus the reflection coefficient of array antenna becomes wider. The sequential rotation of the feeding line of the array antenna can generate axial ration bandwidth which becomes wider than the single one, and every patch generates circular polarization characteristics by continuously having a relative phase of 90 degrees.

The minimum requirement of reflection coefficient, S_{11}, is less than -10 dB, and the bandwidth is more than 0.4 GHz. In order to achieve this requirement, some methods are implemented to the antenna design. One of them is employing Z_S equal to 50 Ω; in this way, it can generate the maximum power of transmission, thus achieved impedance source is equal to load impedance. Investigation of the initial

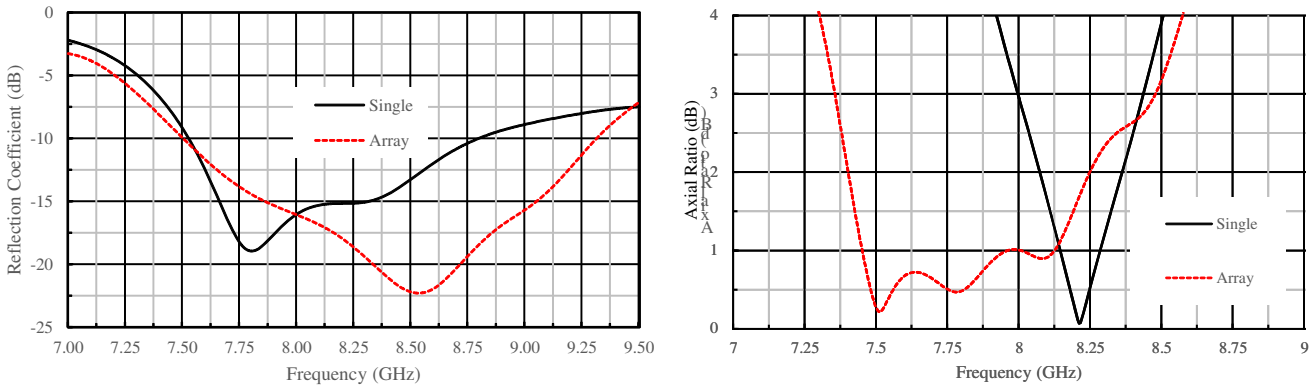

Figure 6. Comparison of simulated result of single and array antenna: (a) Reflection coefficient; (b) Axial ratio.

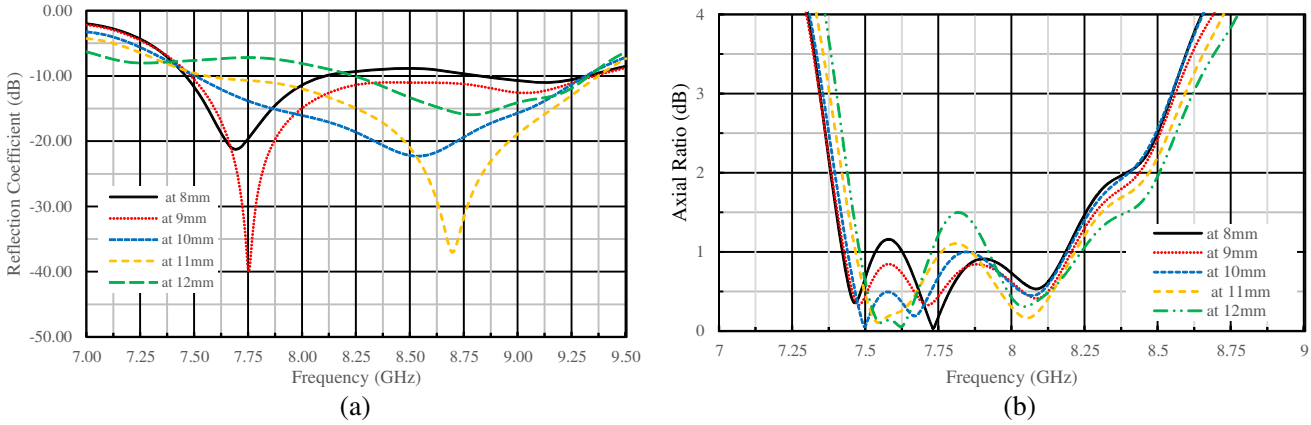

Figure 7. Effect of the feeding line length to: (a) Reflection coefficient, S_{11}, (b) Axial Ratio bandwidth.

result of the microstrip feed path is presented in Figure 7.

Figure 7(a) highlights the alteration of the reflection coefficient, S_{11}, due to variation of the feeding line. Changes are made by varying the length of the feeding line, and then it sweeps from 8 mm, 9 mm, 10 mm, 11 mm, and 12 mm. With length of 8 mm, 8.5% (7.4–8.1 GHz) reflection coefficient, S_{11}, can be obtained. This result is unacceptable. Subsequently, the feeding line is set to 9 mm, and its result shows a progress. Its reflection coefficient, S_{11}, bandwidth reaches 22% (7.5–9.35 GHz). Even though the achievement of the bandwidth is satisfying, its result does not have a decent achievement at the desire frequency. For example, at center frequency of 8.2 GHz nothing but -11.73 dB is obtained. This point is near the minimum requirement of -10 dB, which is unacceptable. Hereinafter, the length of the feeding line to 10 mm and its simulated result shows a better product. The reflection coefficient, S_{11}, bandwidth obtains 21.9% (7.5–9.3 GHz), then at the center frequency of 8.2 GHz it reaches 17.6 dB. The deepest point for this variant is at 8.51 GHz of -22 dB. Another variation of feeding line is set for 11 mm, and its impedance bandwidth reaches 18.9% (7.75 GHz–9.3 GHz), and at the center frequency, -14.3 dB is yielded. Then, the last variation is the feeding line set at 12 mm. Its product shows flatter results. The deepest reflection coefficient, S_{11}, point is at 8.7 GHz of -15 dB, and the achievement of the bandwidth is nothing but 12% (8.25–9.3 GHz). It means that its result is out of the desired frequency. Figures 7(b) and 8 highlight the comparison of the simulated results of the axial ratio and gain. In this case, the variation of feeding line does not give significant influences on the axial ratio and gain. The average bandwidth of all axial ratio results is 13.52%, with the higher percentage of 14.6% and lower one of 12.2%. It means that the gap of each diversity is not significant or almost similar. In addition,

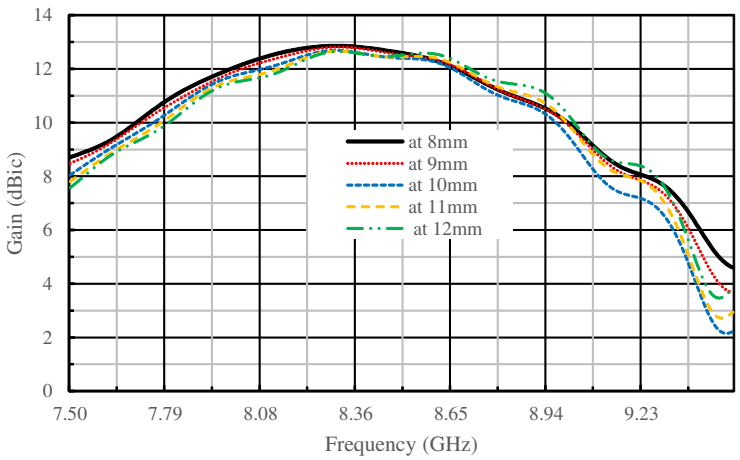

Figure 8. Effect of the feeding line length to the gain.

the gain achievements are also similar to each other. All of the variants achieve more than 12 dBic of gain. The highest peak is at 10 mm, then the lower peak point is at 12 mm. In this section, it can be concluded that the finest variant is when the length of feeding line = 10 mm. A complete summary of investigation is shown in Table 3.

Fabrication process must be accomplished to verify the dependability of the array antenna design. By a proper execution and a good measurement process, the antenna design will be feasible and competent. The investigation on the model of the proposed antenna proceeds on CST Studio Suite 2018, and then the fabrication and measurement are executed in an anechoic chamber at JMRSL of Chiba University. The fabricated antenna is shown in Figure 9, and the total dimension of fabricated antenna is 6 60.92 mm × 60.92 mm. It is fed with an SMA connector at the edge of the substrate. The antenna design is printed on double substrates then put together with plastic screws in every corner. Schematic of the measurement system is shown in Figure 10.

Figure 10 shows the description of the schematic of the measurement system in JMRSL facilities. Some instruments are implemented in the measurement processes. There are two groups of instruments used in this experiment. First one (the instruments set in the anechoic chamber): The turn table for Antenna Under Test (AUT), a pair of conical log spiral antennas (left-handed and right-handed) as a transmitter, and a pole to mount the antenna transmitter. Second one (the equipment that is set outside the anechoic chamber): A controller to control the movement of the turntable, a Vector Network Analyzer (Agilent VNA E8362C) used in this experiment, and a computer unit as data storage and to control all systems.

Table 3. Effect of the feeding line length to reflection coefficient, the axial ratio and gain.

Length of feeding line (mm)	**reflection coefficient, S_{11} (GHz)**	**At center Frequency 8.2 GHz (dB), %**	**Bandwidth AR, (GHz)**	**Gain at the mid-band frequency 8.2 GHz (dBic)**
8	7.4–9.35, 23%	−11.7	7.3–8.5, 14%	12.6
9	7.5–9.35, 22.5%	−11.73	7.3–8.5, 14.6%	12.6
10	7.5–9.3, 21.9%	−17.6	7.3–8.3, 12.2%	12.45
11	7.5–9.3, 21.9%	−14.3	7.3–8.5, 14.6%	12.35
12	8.25–9.5, 12%	none	7.3–8.3. 12.2%	12.26

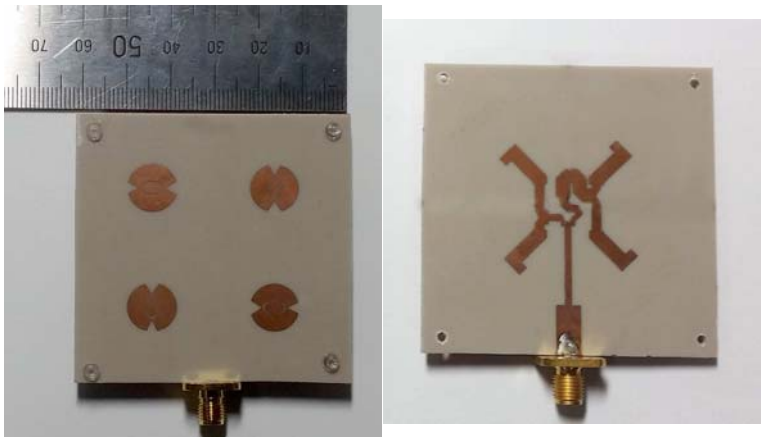

(a) (b)

Figure 9. Fabricated proposed antenna: (a) Patch radiator; (b) Network feeding.

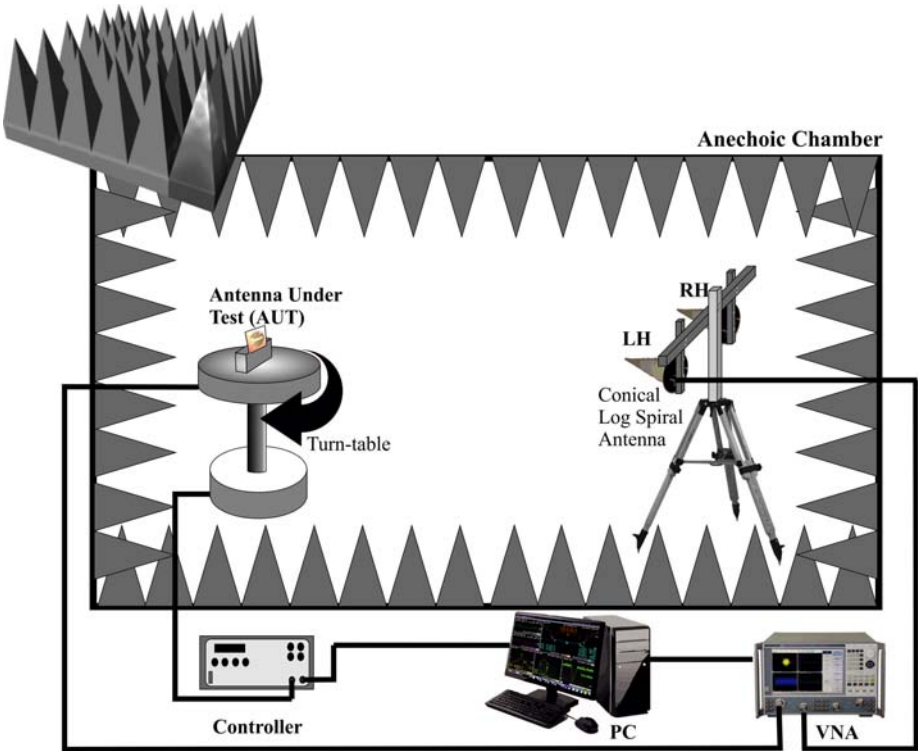

Figure 10. Schematic of measurement system.

Figure 11(a) shows the comparison of simulated and measured reflection coefficients, S_{11}. It displays that there is agreement between simulated and measured impedance bandwidth characteristics. Simulated result can produce the reflection coefficient of 21.9% with low-frequency (8.0 GHz) at 7.46 GHz and its high-frequency (8.4 GHz) at 9.4 GHz. Then, the deepest point of the reflection coefficient is at 8.51 GHz of −22 dB. Nevertheless, in the center frequency (8.2 GHz) it is −17.6 dB. On the other hand, the measured result shows similar characteristics of reflection coefficient, S_{11}. It is 20% with the low-frequency at 7.57 GHz and high-frequency at 9.3 GHz. The deepest point is at 8.09 GHz of −18.12 dB, then in the center frequency 8.2 GHz, it is −16.8 dB. The fabricated antenna produces a good suitability of reflection coefficient, S_{11}, and also a product precision which is at the desired frequency, even though its measured result is decreased for about 1.9%.

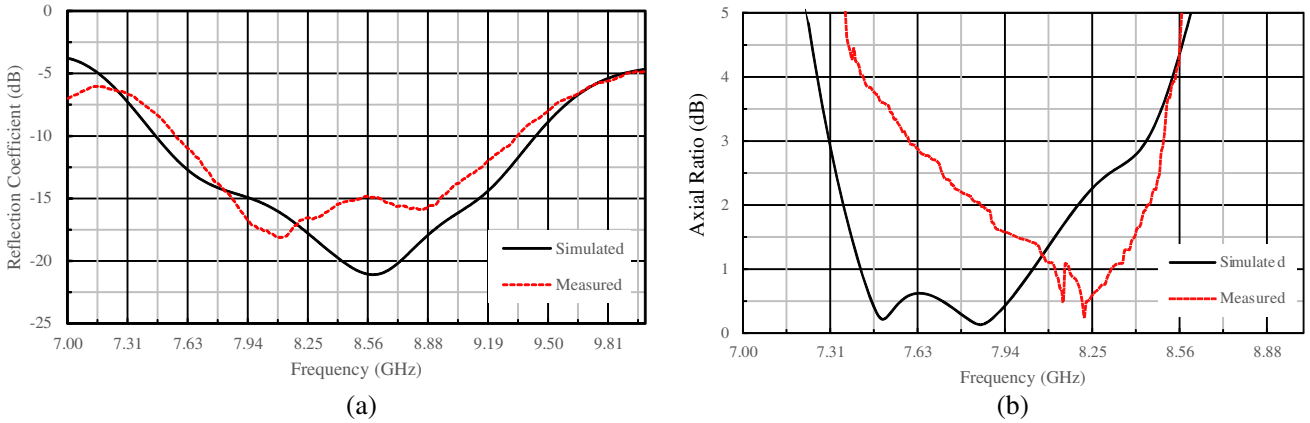

Figure 11. Comparison of simulated and measured results: (a) Reflection coefficient; (b) Axial ratio.

Figure 11(b) depicts a comparison of simulated and measured circularly polarized characteristics. It shows that its simulated result has a wider axial ratio bandwidth than the measured result, obtaining 12.2% with the lower frequency (8.0 GHz) at 7.3 GHz and higher frequency (8.4 GHz) at 8.44 GHz. This simulated result has the deepest point of curve at 7.86 GHz obtaining 0.13 dB, then in the center frequency of 8.2 GHz obtaining 2.09 dB. On the other hand, measured result produces a narrower bandwidth of axial ratio about 11%, with the lower frequency at 7.58 GHz and the higher frequency at 8.5 GHz. This measurement result has the deepest frequency at 8.22 GHz obtaining 0.25 dB, and then in the centre frequency (8.2 GHz) obtaining 0.25 dB. Compared to the simulated one, the measured result is much narrower, but its result has deeper axial ratio and much deeper also at the center frequency, which means that the measurement one is more circularly polarized. In this case, the discrepancies of the results are caused by imprecision in fabrication or some shifting in the fusion between the first and second substrates.

The minimum requirement of the gain is up to 10 dBic. Comparison of simulated and measured gains is shown in Figure 12, which are in agreement with the minimum requirement. In simulated results, 11.14 dBic is obtained at the low frequency (8.0 GHz), while at the high frequency (8.4 GHz) 12.38 dBic is obtained. At the center frequency (8.2 GHz), this antenna design produces 11.8 dBic. Subsequently, the highest gain is at 8.5 GHz which is 12.5 dBic. On the other hand, in measured results, 9.7 dBic is obtained at the low frequency of 8.0 GHz, while at the high frequency (8.4 GHz), 11.65 dBic is obtained. Hereafter, the higher point in this curve at 8.44 GHz is 12.76 dBic. The average values of both gains

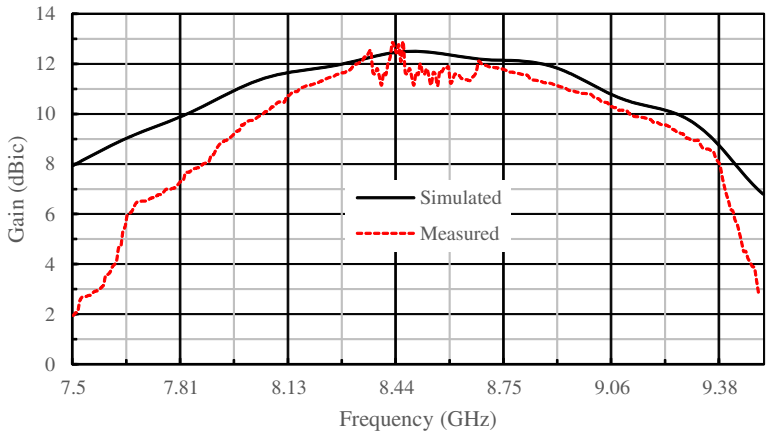

Figure 12. Comparison of simulated result and measured result gain.

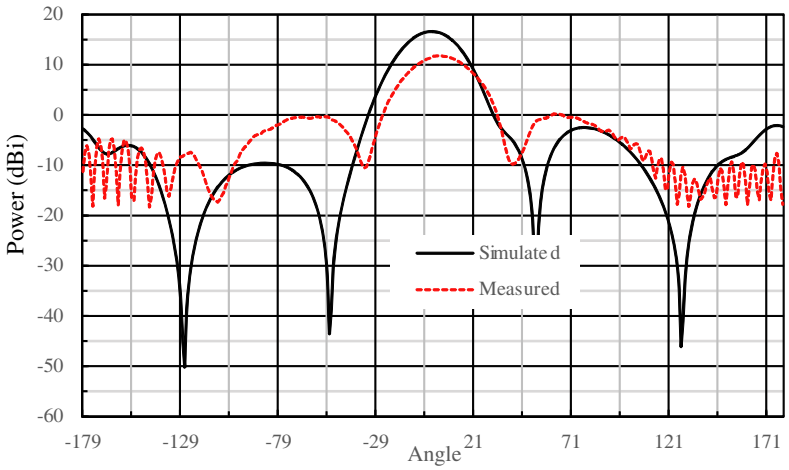

Figure 13. Comparison of simulated and measured radiation pattern of the antenna in cartesian graph.

are similar of 11.81 dBic. This average gain value is calculated from the low frequency of 8.0 GHz to the high frequency of 8.4 GHz. Nevertheless, the achievement of the measured result slightly decreases. The decreasing values or shifted result of the measurement compared to the simulation result is caused by many factors, such as imprecise during fabrication process (cutting, drilling, etching) or error in the measurement process (cabling, program, miss of target) [28].

Simulated and measured radiation patterns of the proposed antenna in Cartesian graph are shown in Figure 13. Its results indicate that the radiation patterns have similarity, although the simulated one shows its power to be stronger than the measured one. The simulated radiation pattern has a main lobe about 16 dBi with the direction at 1°, while the measured result shows that the power of pattern slightly decreases, with its main lobe about 13 dBi. Afterwards, its side lobe level is also higher than the simulated radiation pattern. Nevertheless, the direction is in line with simulated radiation pattern.

In this research, experimentation of the radiation patterns of the proposed antenna is also observed in another polarization. In this case, the proposed antenna has a left-handed circular polarization (LHCP), thus, the opposite polarization is right-handed circularly polarized (RHCP). The purpose of this kind of experimentation is to ensure the exact polarization and the power of radiation. Figure 14 shows the LHCP against RHCP radiation patterns in the X-Z plane and Y-Z plane, 8 GHz, 8.1 GHz, 8.2 GHz, 8.3 GHz, and 8.4 GHz. The direction of maximum radiation pattern tends to get tilting about 1 degree in the case of X-Z plane. This state is similar to the simulation one. Overall, the fabricated antenna has a good agreement with the minimum requirement.

To complete the investigation and show its dependabilities, this section also provides comparison between the proposed antenna design and other designs, as shown in Table 4. It shows that 2×2 array antenna with sequential rotation feeding line has wider axial ratio bandwidth and higher gain than the other models.

Table 4. Comparison antenna design.

Antenna Design	S_{11} BW (GHz)	<3 dB Axial Ratio BW (dB), %	Gain (dBic)
CP Array Ant. for X-band	21,9% (7.5–9.3)	14.6% (7.3–8.5)	12.35
Model 1 [29]	25% (5.3–6.85)	14% (5.45–6.3)	6.3
Model 2 [30]	24% (2.69–3.4)	4.7% (2.91–3.05)	12.4
Model 3 [31]	83% (4–9) Ripple	4% (4.8–7.2)	10.5

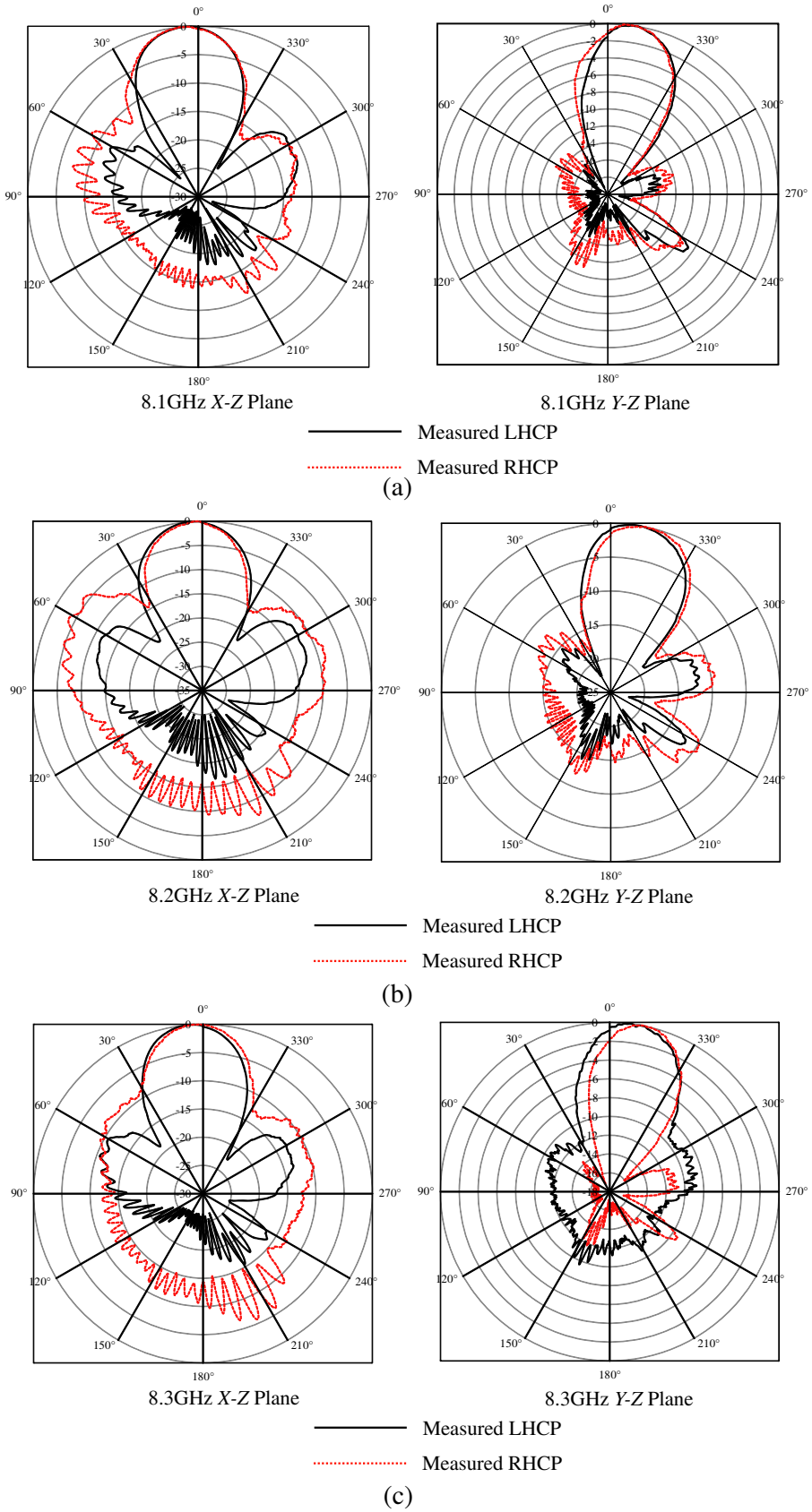

Figure 14. Measured and simulated radiation pattern in polar graph: (a) 8.1 GHz; (b) 8.2 GHz; (c) 8.3 GHz.

4. CONCLUSION

A CP microtrip 2×2 array antenna with triangle truncation factor for X-band communication is proposed in this research. This antenna uses sequential rotation methods in its design, with the relative phases of 0°, 90°, 180°, and 270°. This antenna has a total dimension of 60.92 mm × 60.92 mm. The fabrication and measurement result indicate that the proposed antenna is in agreement with the simulation result and the minimum requirement. Its measurement result of reflection coefficient, S_{11}, yields 20%, which is lower than the simulated result about 1.9%. Afterwards, the axial ratio bandwidth reaches 11%; however, the measured result is 1.2% lower than simulated result. Nevertheless, the measured result in the center frequency is better than the simulated one. In average value, the simulated and measured results of gain are the same, standing at 11.81 dBic. Its gain result shows good characteristics. The simulation and measurement have decent results and are in agreement with the minimum requirement. However, the measured result shows a slight decrease compared to the simulation one, due to the imprecise fabrication (drilling, cutting, etching, etc) or error in measurement process (cabling, losses in system, etc). Overall, this entire antenna design is acceptable and excellent.

ACKNOWLEDGMENT

This work was supported in part by the European Space Agency (ESA) Earth Observation Category 1 under Grant 6613; the Japanese Government National Budget — Ministry of Education and Technology (MEXT) FY2015-2017 under Grant 2101; Chiba University Strategic Priority Research Promotion Program FY2016-FY2018; Chiba University Institute of Global Prominent Research FY2016-FY2018; and Indonesian National Institute of Aeronautics and Space (LAPAN) under Lapan-Chibasat Microsatellite SAR project; Indonesian National Institute of Aeronautics and Space (LAPAN), and Ministry of Research, Technology and Higher Education of the Republic of Indonesia for supporting all our activities.

REFERENCES

1. Lee. K. and K. Tong, "Microstrip patch antennas — Basic characteristics and some recent advances," *Proceedings of the IEEE*, Vol. 100, 7, July 2012.
2. James. J. R. and P. S. Hall, *Handbook of Microstrip Antenna*, Peter Peregrinus Ltd, London, UK, 1989.
3. Kabacik. P. and M. Bialkowski, "Microstrip patch antenna design considerations for airborne and spaceborne application," *IEEE Antenna and Propagation Society International Symposium)*, Atlanta, USA, 1989, 10.1109/APS.1998.701628.
4. Chen. X., L. Yang, J. Zhao, and G. Fu, "High-efficiency compact circularly polarized microstrip antenna with wide beamwidth for airborne communication X," *IEEE Antennas and Wireless Propagation Letter*, Vol. 15, 1518–1521, 12 January 2016, 10.1109/LAWP.2016.2517068.
5. Vazquez-Roy, J. L., V. Krozer, and J. Dall, "Wideband dual-polarization microstrip patch antenna array for airborne ice sounder," *IEEE Antennas and Propagation Magazine*, Vol. 54, 98–107, 4 August 2012, 10.1109/MAP.2012.6309160.
6. Chakravorty. D., S. K. Singh, P. Singh, et al., "Dual band triangular patch antenna for land & maritime military communication system and WLAN5.8 GHz application," *IEEE IEMCON 8th* Vancouver, Canada, November 2017, 10.1109/IEMCON.2017.8117227.
7. Tofigh. F., J. Nourinia, M. Azarmanesh, and K. M. Khazaei, "Near-field focused array microstrip planar antenna for medical applications," *IEEE Antennas and Wireless Propagation Letter*, Vol. 13, 951–954, 16 May 2014, 10.1109/LAWP.2014.2322111.
8. Mall. L. and R. B. Waterhouse, "Simple, small antenna terminal for maritime satellite communications," *IEEE Electronics Letter*, Vol. 40, 646–648, 07 June 2004, 10.1049/el:20040462.
9. Kurniawan. F, J. T. Sri Sumantyo, and A. Munir, "Effect of truncation shape againt axial ratio of left-handed circularly polarized X-band antenna," *The 15th Quality in research (QIR))*, Baly, 2017.

10. Kurniawan. F, J. T. Sri Sumantyo, S. Gao, K. Ito, and C. E. Santosa, "Square-shaped feeding truncated circularly polarised slot antenna," *IET Microwave, Antenna and Propagation*, 10.1049/iet-map.2017.0805, 05 February 2018, 10.1049/el:20040462.
11. Waterhouse, R. B., *Microstrip Patch Antenna: A Designer's Guide*, Kluwe Academic Publisher, Boston/ Dordrecht/ London, 2003.
12. Wang, Y., "A series feed E-shaped microstrip antenna with high gain," *ISAPE, 2012 10th International Symposium*, 13243957, Xiang, China, 2013, 10.1109/ISAPE.2012.6408737.
13. Tan, W., Z. Shen, Z. Shao, and M. Fujise, "A gain-enhanced microstrip-fed cavity-backed slot antenna," *APMC 2005*, 8874417, Suzhou, China, 2005, 10.1109/APMC.2005.1606383.
14. Jia, J., C. Lu, and Y. Jie, "Design of broadband circularly polarized high gain microstrip antenna with L-shaped probe feed," *International Conference on Microwave and Millimeter Wave Technology (ICMMT)*, Shenzhen, China, 2012, 10.1109/ICMMT.2012.6230173.
15. Juyal, P. and L. Shafai, "A high-gain single-feed dual-mode microstrip disc radiator," *IEEE Trans. on Antennas and Propagation*, Vol. 64, No. 6, 2115–2126, June 2016, 10.1109/TAP.2016.2543804.
16. Suthar, H., et al., "Gain enhancement of microstrip patch antenna using near-zero index metamaterial (NZIM) lens," *Twenty first National Confrence on Communication*, Mumbai, India, March 2015, 10.1109/NCC.2015.7084840.
17. Mollaei, M. S. M., E. Zangenh, and M. F. Farahani, "Enchancement of patch antenna cain using cylincrical shell-shaped superstrate," *IEEE Antenna and Wireless Propagation Letter* Vol. 16, 2570–2573, 2017.
18. Ta, S. X. and T. K. Nguyen, "AR bandwidth and gain enhancements of path antenna using single dielectric superstrate," *Electronic Letters*, Vol. 53, No. 15, 1015–1017, 7 20 2017.
19. Pal, A., A. Mehta, R. Lewis, and N. Clow, "Reconfigurable phased array antenna enabling a high gain wide angle beam scanning," *2015 IEEE International Symposium on Antennas and Propagation and USNC/URSI National Radio Science Meeting*, Vancouver, BC, Canada, Oct. 2015, 10.1109/APS.2015.7305492.
20. Yang, W., J. Zhou, Z. Yu, and L. Li, "Bandwidth and gain enhanced cirrularly polarized antenna array using sequential phase feed," *IEEE Antennas and Wireless Propagation Letters* Vol. 13, 1215–1218, Jun. 2015.
21. Stutzman, W. L. and G. A. Thiele, *Antenna Theory and Design*, 2nd Edition, Wiley, US, 1998.
22. Balanis, C. A., *Modern Antenna Handbook*, Wiley, US, 2008.
23. Caso, R., et al., "A novel dual-feed slot-coupling feeding technique for circularly polarized patch arrays," *IEEE Antennas and Wireless Propagation Letters*, Vol. 9, 183–186, March 2010.
24. Kaffash, S. and M. Kamyab, "A sequentially rotated RHCP stacked patch antenna array for INMARSAT-M land applications," *6th European Conference on Antennas and Propagation (EUCAP)*, 12771959, Prague, Czech Republic, March 2012.
25. Kraft, U. R., "An experimental study on 2×2 sequential-rotation arrays with circularly polarized microstrip radiators," *IEEE Trancs. on Antenna and Propagation*, Vol. 45, No. 10, 1459–1466, October 1997.
26. Chen, A., Y. Zhang, Z. Chen, and C. Yang, "Development of a Ka-band wideband circularly polarized 64-element microstrip antenna array with double application of the sequential rotation feeding technique," *IEEE Antennas and Wireless Propagation Letters*, Vol. 10, 1270–1273, Noveber 2011.
27. Kurniawan, F., T. Sri Sumantyo, A. Bintoro, and D. A. Purnamasari, "Bandwidth enhancement of circular polarized X-band microstrip array antenna using ERS," *2017 IEEE CAMA*, December 2017, 10.1109/CAMA.2017.8273409.
28. Kurniawan, F., J. T. Sri Sumantyo, and A. Munir, "Wideband LHCP truncated-circular-shape microstrip antenna for SAR application," *IEEE International Symposium on Antennas and Propagation (AP-S)*, San Diego, July 2017.
29. Maddio, S., "A circularly polarized antenna array with a convenient bandwidth/size ratio based on non-identical disc elements," *Progress In Electromagnetics Research Letters*, Vol. 57, 47–54, 2015.

30. Han, T. Y., "Series-fed microstrip array antenna with circular polarization," *Hindawi: International Journal of Antennas and Propagation*, Article ID 681431, 2012.
31. Liu, C., A. Yan, C. Yu, and T. Xu, "Improvement on a 2×2 elements high gain circularly polarized antenna array," *Hindawi: International Journal of Antennas and Propagation*, Article ID 252717, 2015.